A general model for the helical structure of geophysical flows in channel bends

M. Azpiroz-Zabala[1,2]*, M.J.B. Cartigny[3], E.J. Sumner[1], M.A. Clare[2], P.J. Talling[3], D.R. Parsons[4], C. Cooper[5]

[1] Ocean and Earth Sciences, University of Southampton, European Way, SO14 3ZH Southampton, UK

[2] National Oceanography Centre, Southampton, European Way, SO14 3ZH Southampton, UK

[3] Departments of Earth Sciences and Geography, University of Durham, DH1 3LE Durham, UK

[4] Department of Geography, Environment and Earth Sciences, University of Hull, Cottingham Road, HU6 7RX Hull , UK

[5] formerly at Chevron Energy Technology Company, 6001 Bollinger Canyon Road, San Ramon, CA 94583 USA

[*] Corresponding author: Maria Azpiroz-Zabala (m.azpiroz@soton.ac.uk)

Key Points:

- First direct measurements of the helical flow structure of turbidity currents as they travel around a bend.
- Turbidity currents of different thicknesses and velocities exhibit the same helical flow structure.
- We reconcile current controversy with a new model that explains helical flow structure for a wide range of geophysical flows.

Abstract

Meandering channels host geophysical flows that form the most extensive sediment transport systems on Earth (i.e. rivers and submarine channels). Measurements of helical flow structures in bends have been key to understanding sediment transport in rivers. Turbidity currents differ from rivers in both density and velocity profiles. These differences, and the lack of field measurements of turbidity currents, have led to multiple models for their helical flow. Here we present the first measurements of helical flows from turbidity currents in the ocean. These ten flows lasted between one and ten days, had up to ~80-metre thickness, and all displayed the same helical structure. This structure comprised two vertically-stacked cells, with the bottom cell rotating with the opposite direction to helical flow in rivers. Furthermore, we propose a general model that predicts the range of helical flow structures observed in rivers, estuaries and turbidity currents based on their density stratification.

1 Introduction

Extensive submarine channels transport billions of tonnes of sediment over hundreds of kilometres, and they form vast sedimentary deposits (called submarine fans) in the deep sea (Shepard, 1933; Normark, 1970; Savoye et al., 2009). The largest submarine fans (e.g. Amazon, Bengal, Indus, Congo fans) are fed by meandering, rather than straight submarine channels, suggesting that bends may enhance distances over which sediment is transported. Submarine channels host episodic sediment-laden gravity currents called turbidity currents. Individual turbidity currents are capable of transporting more sediment than the annual discharge of rivers worldwide (Talling et al., 2007). There are few direct observations of deep-sea turbidity currents (Khripounoff et al., 2003; Vangriesheim et al., 2009; Talling et al., 2015; Cooper et al., 2016). Before collection of the data presented here (Cooper et al., 2013, Azpiroz-Zabala et al., in press), there were no detailed (sub-minute) measurements from within a meander bend. Instead, our understanding of sediment transport processes in meandering deep-sea channels was based on uncalibrated experimental and numerical models, or by comparison to rivers or saline density flows.

Rivers, channelized estuaries and saline underflows show a helical flow structure when passing through a bend. This helical structure can be broken into down-stream and cross-stream components (Rosovskii, 1957; Nidzieko et al., 2009; Parsons et al., 2010; Sumner et al., 2014). The helical structure is caused by the variability of the centrifugal acceleration acting on the flow as it travels around a bend. The centrifugal acceleration induces varying pressure gradients resulting from superelevation of the flow at the outer bend, which can generate counter-acting pressure gradients as a result of cross-channel density variation, i.e. stratification, of the flow (Rozovskii, 1957; Thorne et al., 1985; Sumner et al., 2014). The magnitude and rotation direction of the helical flow strongly influences sediment processes that control erosion and deposition within a channel. Hence, helical flow has been invoked as a fundamental control on how channel systems evolve (Rozovskii, 1957; Thorne et al., 1985; Peakall et al., 2000).

Previous work has demonstrated that the helical structure can vary in two key ways. First, it can vary in the direction of rotation. Second, there can be a single helix (i.e. one rotating cell), or multiple helices stacked on top of one another (e.g. Corney et al., 2006; Imran et al., 2008; Corney et al., 2008). Helical circulation in rivers is dominated by a single helix that rotates in a clockwise direction when looking in a downstream direction at a left-hand bend. (Rozovski, 1957; Thorne et al., 1985). Initial numerical models suggested that circulation that is similar to a river bend would also occur for turbidity currents (Kassem and Imran, 2004). However, the first physical experiments of helical circulation in turbidity currents showed an opposite direction of rotation – with the near-bed flow moving towards the outer bank (Corney et al., 2006; Keevil et al., 2006). To complicate matters further, both directions of helical circulation (river-like and river-reversed) have subsequently been observed in turbidity current experiments and models, depending on flow conditions and channel morphology conditions (Imran et al., 2007; Islam and Imran, 2008; Cossu and Wells, 2010; Abad et al., 2011; Giorgio Serchi et al., 2011; Huang et al., 2012; Dorrell et al, 2013; Janocko et al., 2013; Bolla Pittaluga and Imran, 2014; Ezz and Imran, 2014).

Flow around bends in well-mixed estuaries show a river-like basal helical circulation, while stratified estuaries and saline flows are river-reversed (Nidzieko et al., 2009; Wei et al., 2013). In stratified flows, across-flow variation in stratification (i.e. flow density) sets up an additional lateral pressure gradient that is thought to play a key role in the direction of the flow rotation (Nidzieko et al., 2009; Sumner et al., 2014). Such stratification-triggered pressure gradients have been suggested to be important for turbidity currents, which are stratified because of their vertical variation in sediment concentration and hence density (Sumner et al., 2014; Peakall and Sumner, 2015). This hypothesis has not yet been tested because of a lack of field-scale observations of turbidity currents.

Here we present the first direct measurements of turbidity currents at a meander bend in the ocean, including ten flows with varying flow conditions. We use this data to determine the rotation direction of helical flow within these turbidity currents. This provides the first field test of existing numerical and experimental models. Second, we determine how flow structure varies with fluctuating flow properties, and discuss the implications for the morphodynamic evolution of submarine channel bends. Finally, we compare our results with existing field measurements of helical flows in other geophysical flows. We propose a general model that can predict helical flow structure across a wide range of geophysical flows including rivers, saline density flows, and turbidity currents.

2 Study area

Our field measurements were recorded at 2,000 m water depth in the Congo Canyon (Cooper et al., 2013; Azpiroz-Zabala et al., in press). The Congo Canyon is the proximal section of one of the largest submarine channel systems on Earth, and it is fed directly by the Congo River (Heezen et al., 1964). The submarine channel extends for more than 1000 km, from the continental shelf to its termination in a large submarine fan in 5000 m water depth (Heezen et al., 1964; Khripounoff et al., 2003). Over its upper course, the Congo Canyon has a meandering planform with tight bends, a deeply incised thalweg and numerous terraces (Fig. 1). The Congo Canyon is a highly active system in the present day. There are several turbidity currents each year in the upper canyon, based on telecommunication cable breaks (Heezen et al., 1964) and direct flow measurements (Khripounoff et al., 2003; Cooper et al., 2013; 2016; Azpiroz-Zabala et al., in press).

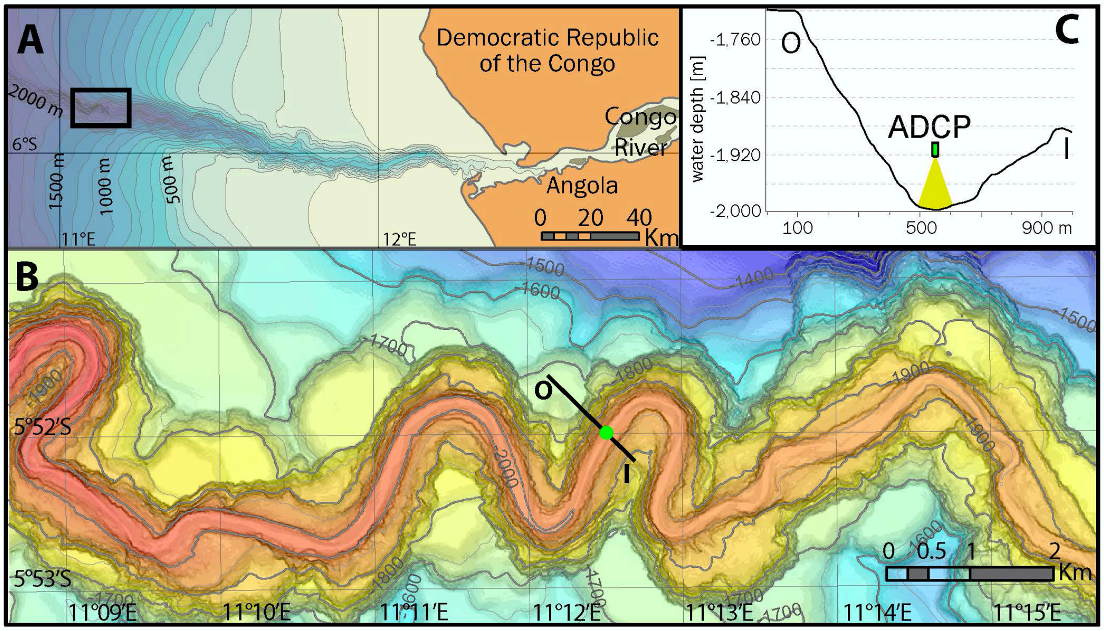

Figure 1. Location of the ADCP in the Congo Canyon. (a) Map of the Congo Canyon showing the study area (rectangle), with bathymetric contours in meters. (b) Detailed map showing the location of the instrumented mooring (green circle). Bold line indicates cross-canyon profile in panel 1c. I and O denotes inner bend and outer bend respectively. (c) Cross-canyon profile at deployment location showing acoustic Doppler current profiler (ADCP) suspended 85 m above the canyon floor.

3 Methods

The dataset re-analysed here represents the first detailed direct measurements of turbidity currents in the deep ocean (Cooper et al., 2013; Azpiroz-Zabala et al., in press). Ten flows were measured, with flow durations ranging between eight hours to more than nine days. Flow thicknesses varied from 16 m to 75 m; and flow velocities reached up to 2.3 m/s (Azpiroz-Zabala et al., in press).

The data were collected using a 300 kHz acoustic Doppler current profiler (ADCP) anchored downstream of a meander bend in the Congo Canyon (Fig. 1). The ADCP emits acoustic signals into the water column, and computes flow velocities based on the Doppler shift in the returned signal that bounces off particles within the flow. The ADCP was downward looking, and moored 85 m above the seafloor from December 2009 to March 2010 (Fig. 1). Velocities were measured every five seconds and were vertically averaged over two-metre high grid cells (Cooper et al., 2013).

We deduce the helical circulation from the vertical velocity profiles measured by the ADCP by calculating primary and secondary velocities. We define primary velocity as follows: we evaluate the flow direction for each ADCP velocity measurement binned by depth, and average the velocities in this vertical profile to obtain the mean flow velocity direction. The primary velocity is then the component of velocity parallel to the mean velocity direction. We then define secondary velocity as the component of the velocity measurements perpendicular to the mean velocity direction (Rozovskii, 1957). In a similar way to previous studies of helical flows based on measurements from single moorings, we use the secondary velocity to infer the helical flow structure (Nidzieko et al., 2009). The sign of the secondary velocity represents the direction of the secondary flow captured by the ADCP. Positive is towards the outer bend, and negative is towards the inner bend. The Rozovskii definition of secondary circulation assumes that the total outward directed velocity is balanced by an equal total inwards directed velocity. These secondary flow vectors define cells that provide a two-dimensional view of the helical flow in the across-flow section (Fig. 2).

The ADCP data were processed using the following steps (see Supporting Information for more detail): (1) Data was linearly interpolated from velocities of 0 m/s at the seabed to the velocity value of the lowest reliable measurement at 5 m above the seafloor; (2) The resultant vertical velocity profiles were depth-averaged (Ellison and Turner, 1959) to obtain the average flow velocity and depth; (3) Primary and secondary velocities were calculated respectively as parallel and perpendicular to this average flow direction using the Rozovskii method (Rozovskii, 1957); (4) Results were averaged over 30 minutes to reduce sampling deviation of measurements. (5) Profiles influenced by tidal currents of magnitudes close to the secondary velocities were removed; (6) patterns of helical flow were analysed by arranging the data by flow thickness.

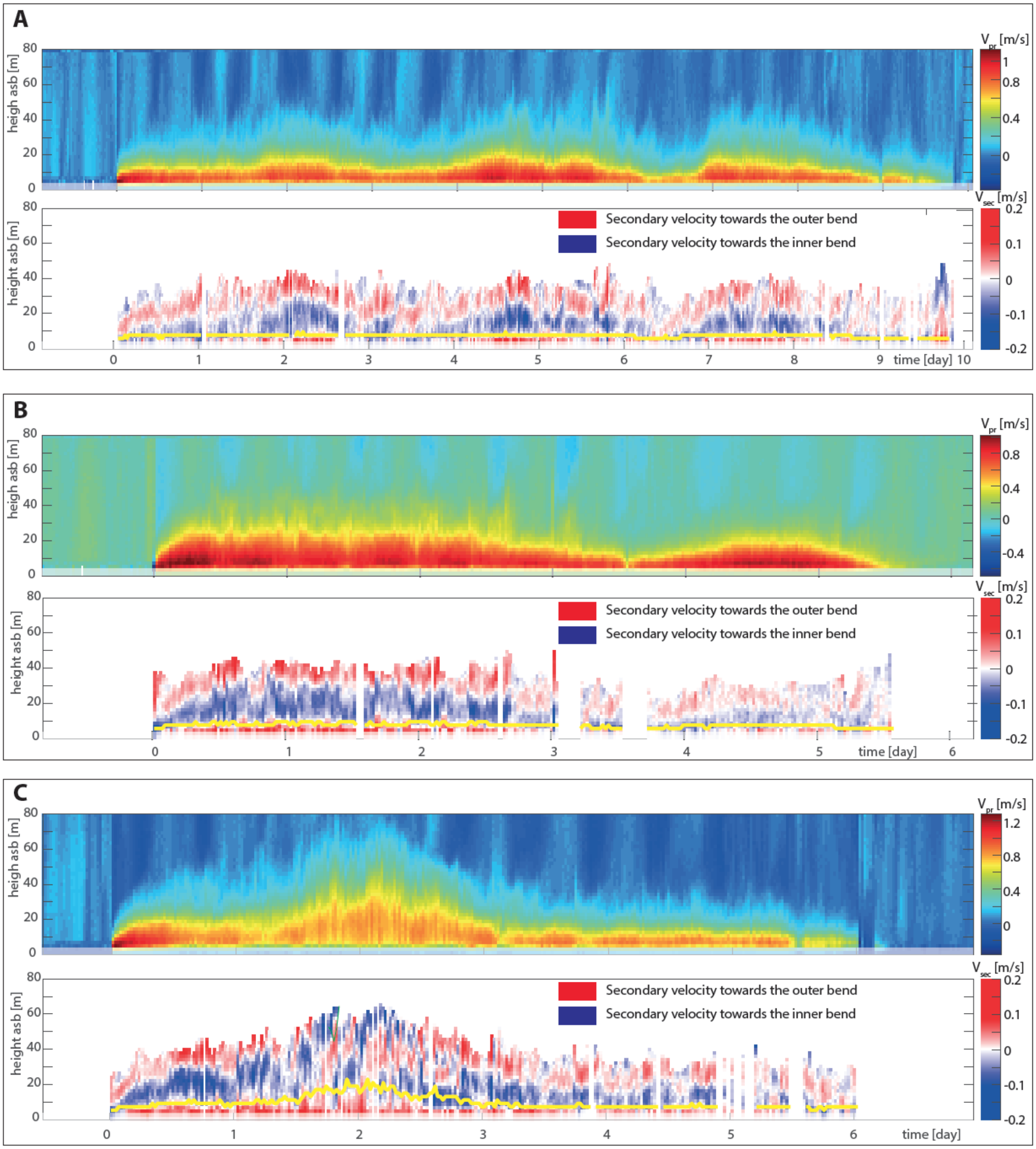

Figure 2. Primary (top) and secondary (bottom) velocities for three events recorded in the Congo Canyon. (a) Flow 1, which is the longest duration flow. (b) Flow 4, the flow that shows a most stable secondary circulation structure. (c) Flow 10, the fastest flow entirely recorded. Positive values denote motion towards the outer bend, and negative values denote motion towards the inner bend. Yellow lines in secondary velocity panels indicate height above the seabed (asb) of maximum velocity. Side lobe interference area is shaded off at the bottom of each panel. Blank strips in secondary velocity panels define areas of strong tidal currents.

4 Results

For the first time, we can visualise and quantify helical flow in field-scale turbidity currents (Fig. 2). The ten measured flows vary considerably in maximum thickness, duration and maximum primary velocity. Surprisingly, despite these variations, the secondary circulation pattern remains consistent (Fig. 3). The secondary circulation consists of two vertically stacked cells, and this structure is independent of primary velocity and flow thickness (at least for flows <52 m thick; Fig. 3). The lower cell rotates in a river-reversed direction, counter-clockwise when looking in a downstream direction, whilst the upper cell has the opposite direction of motion (Fig. 2). The average secondary flow profile has maximum velocities from 0.02–to 0.09 m/s, which are 2-5% of the corresponding flow maximum velocity. The magnitude of secondary circulation is lower for flows between 26 m and 34 m in thickness, but the same two-cell pattern holds. In all cases, the centre of the lowermost circulation cell corresponds to the height of the maximum primary flow velocity.

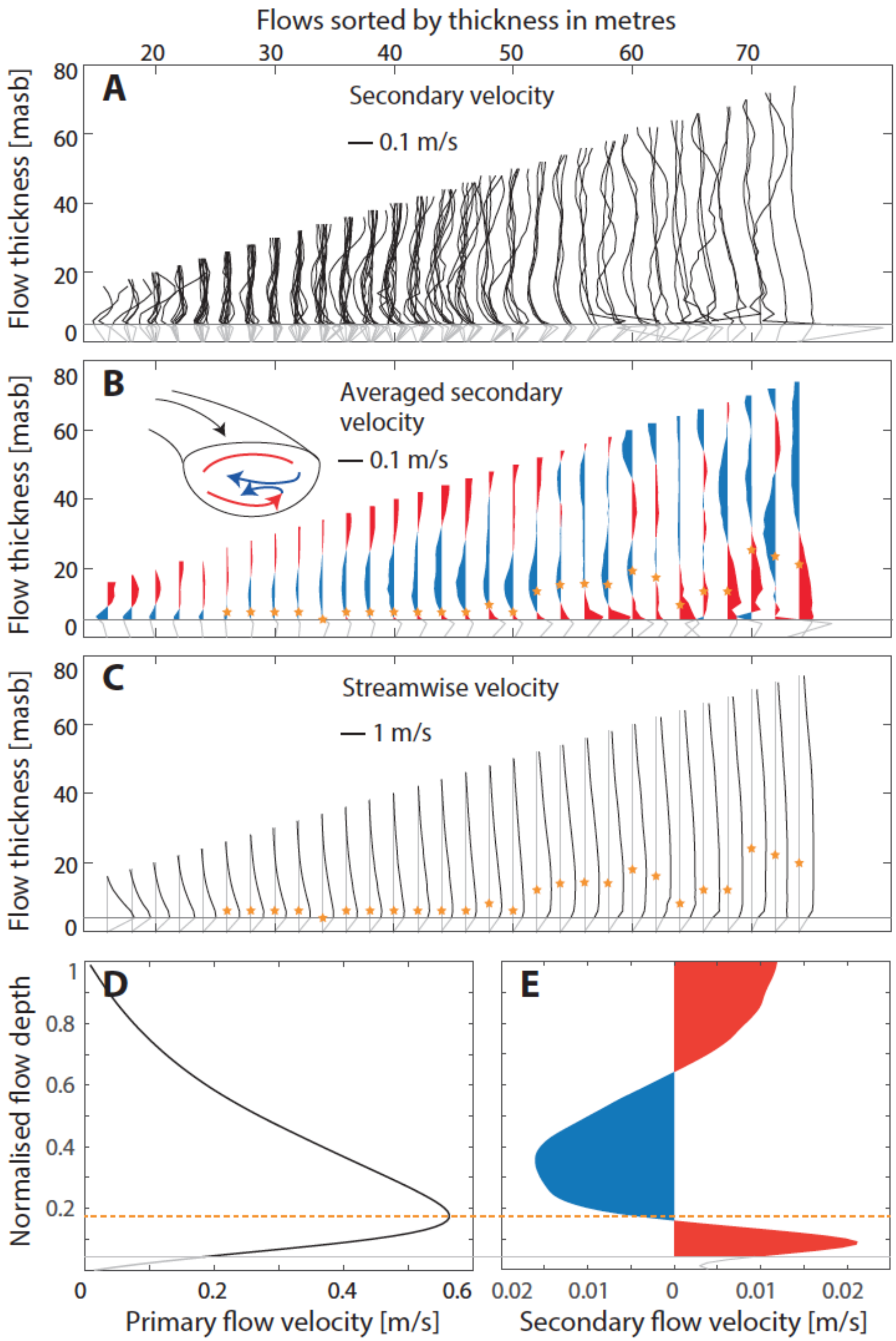

Figure 3. Averaged profiles of primary and secondary velocity profiles according to flow thickness. (a) Event-averaged secondary velocity profiles arranged by their flow thickness. The

yellow stars indicate the height of the maximum primary velocity. Profiles in side lobe interference area are shown in grey. Horizontal grey line marks top of side lobe interference area. (b) Average of profiles shown in (a). Red colours denote positive secondary velocities, towards the outer bend. Blue colours denote negative secondary velocities, towards the inner bend. (c) Event-averaged primary velocity profiles arranged by their flow thickness. (d) Depth-normalised primary velocity profile, and (e) depth-normalized secondary velocity profile constructed by averaging over all available measurements. Normalisation has been calculated according to flow depth. Masb in x-axis in (a)-(c) denotes metres above seabed.

5 Discussion

5.1. What controls the rotation direction of helical flow?

Circulation cells are formed predominantly by the interaction of two pressure gradients (Fig. 4). In river-like circulation, centrifugal forces drive superelevation of the upper surface of a flow towards the outer bend, generating a pressure gradient due to the inclined water surface elevation that drives near-bed flow towards the inner bend. In the case of stratified saline density flows, an additional counter-acting pressure gradient is generated by dense fluid accumulating in the inner bend, which sets up a lateral pressure gradient that drives near-bed flow towards the outer bend (Fig. 4) (Nidzieko et al., 2009; Umlauf and Arneborg, 2009; Sumner et al., 2014). Where the stratification-triggered pressure gradient dominates, near-bed fluid is forced back towards the channel axis in a river-reversed direction of rotation (Nidzieko et al., 2009; Umlauf and Arneborg, 2009; Sumner et al., 2014). It has previously been hypothesized that a similar mechanism might occur in sediment-laden turbidity currents (Sumner et al., 2014) – our new data provides the first field evidence from turbidity currents measured in the deep-sea to support this hypothesis.

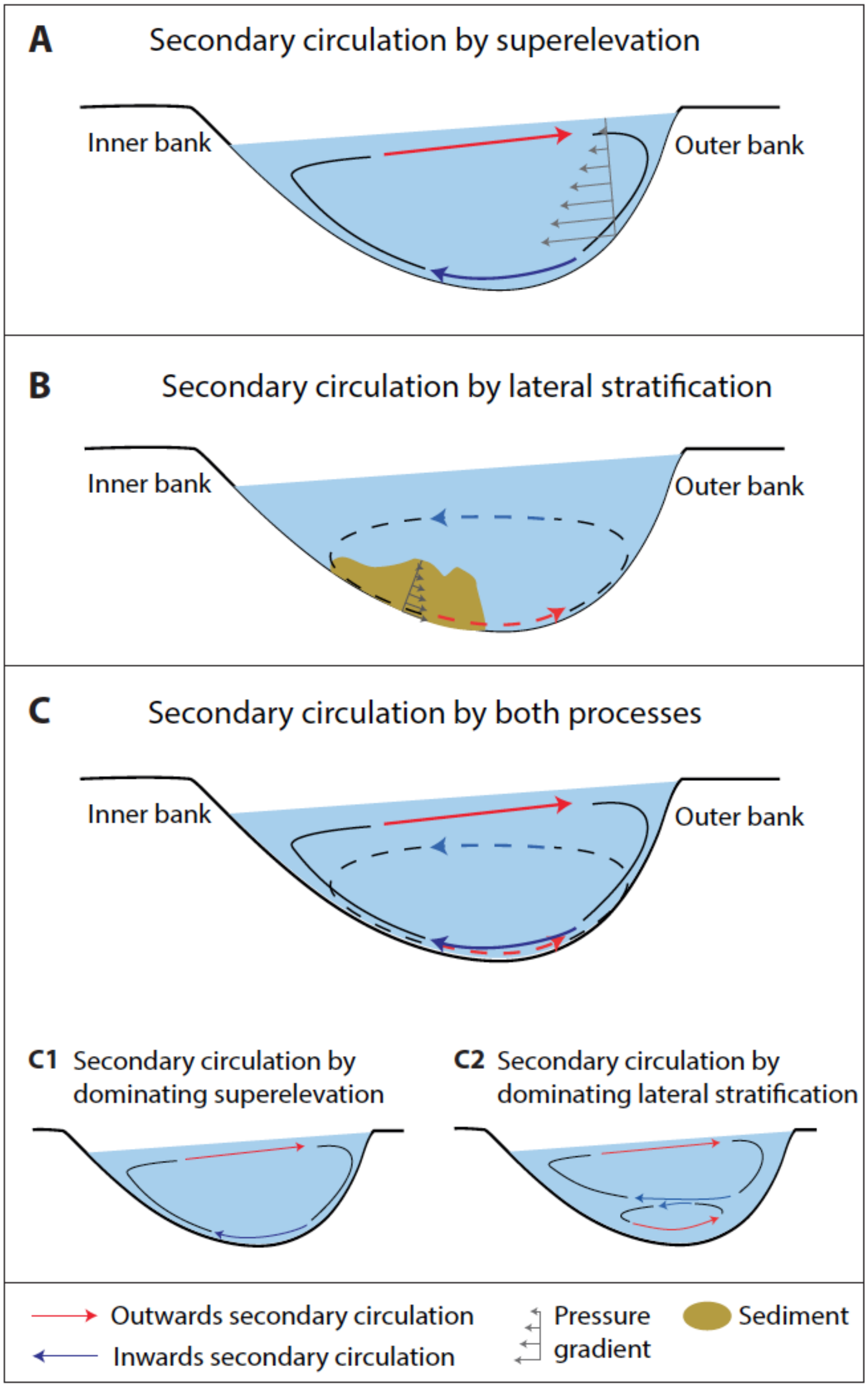

Figure 4. Schematic drawings of cells of secondary circulation produced by pressure gradients. (a) Circulation cell and pressure gradients by superelevation caused by centrifugal forces only, (b) Circulation cell and pressure gradients by lateral flow stratification only, and (c) Combination of secondary circulation cells in (a) and (b). (c1) and (c2) show secondary circulation cells for two scenarios of pressure gradient by superelevation versus pressure gradient by lateral stratification. In (c1) pressure gradient by superelevation dominates; in (c2) pressure gradient by lateral stratification dominates.

5.2. Development of the existing helical flow model based on the new data from turbidity currents

Our flow measurements come from a mooring located downstream of the bend apex (Fig. 1). Therefore, the measurements reflect the evolution of the processes operating within the bend. As the flow travels around the bend, it experiences a centrifugal force that causes superelevation of the flow towards the outer bend, which generates a pressure gradient towards the inner bend (Fig. 4). This results in a single, river-like, helical cell that pushes the majority of the sediment carried by the turbidity current to the inner bend. The accumulation of sediment-laden fluid at the inner bend results in a lateral pressure gradient that opposes the flow of sediment-laden fluidwards the inner bend. Just downstream of the apex, the centrifugal acceleration decreases and as a result the inwardly directed pressure gradient (caused by superelevation) also decreases. Thus, the outwardly directed pressure gradient (caused by stratification) equals the original superelevation-driven force and cross-stream near-bed flow must stop before switching to being outwardly directed as the centrifugal forces start to decrease (Fig. 4). Our model contrasts with earlier models that proposed switching of flow direction occurred between bends. Also, rather than reversing the original direction of the flow cell, this process spawns a new river-reversed near-bed flow cell. This river-reversed flow cell is located beneath the original river-like flow cell (Nidzieko et al., 2009). This results in a two-cell structure. The upper cell is driven by pressure gradients due to flow superelevation, and the lower cell driven by pressure gradients due to lateral stratification within the flow (Fig. 2 and 3). The thickness of the bottom cell is controlled by the height to which the sediment is elevated when pushed towards the inner bend. We observe a correlation between the height of maximum downstream velocity and the centre of the bottom cell. This correlation is probably because it is difficult for sediment to mix across a low turbulence zone that occurs near the velocity maximum of a turbidity current (Eggenhuisen and McCaffrey, 2012).

5.3. A general model for helical flow

In this section we demonstrate that the model described above can be further extended to predict helical flow structure in a diverse array of geophysical flows from rivers to saline density flows and turbidity currents.

All of these flows experience centrifugally-driven superelevation of their upper surface. This superelevation creates a pressure gradient that causes river-like helical flow, with inwardly directed near-bed flow (Figs. 4, 5). This can cause the accumulation of dense fluid or sediment towards the inner bend, which creates lateral stratification, and causes an opposing pressure gradient back towards the outer bend (Fig. 4). We suggest that three potential scenarios may exist (A, B and C in Fig. 5), depending on the relative dominance of these two pressure gradients.

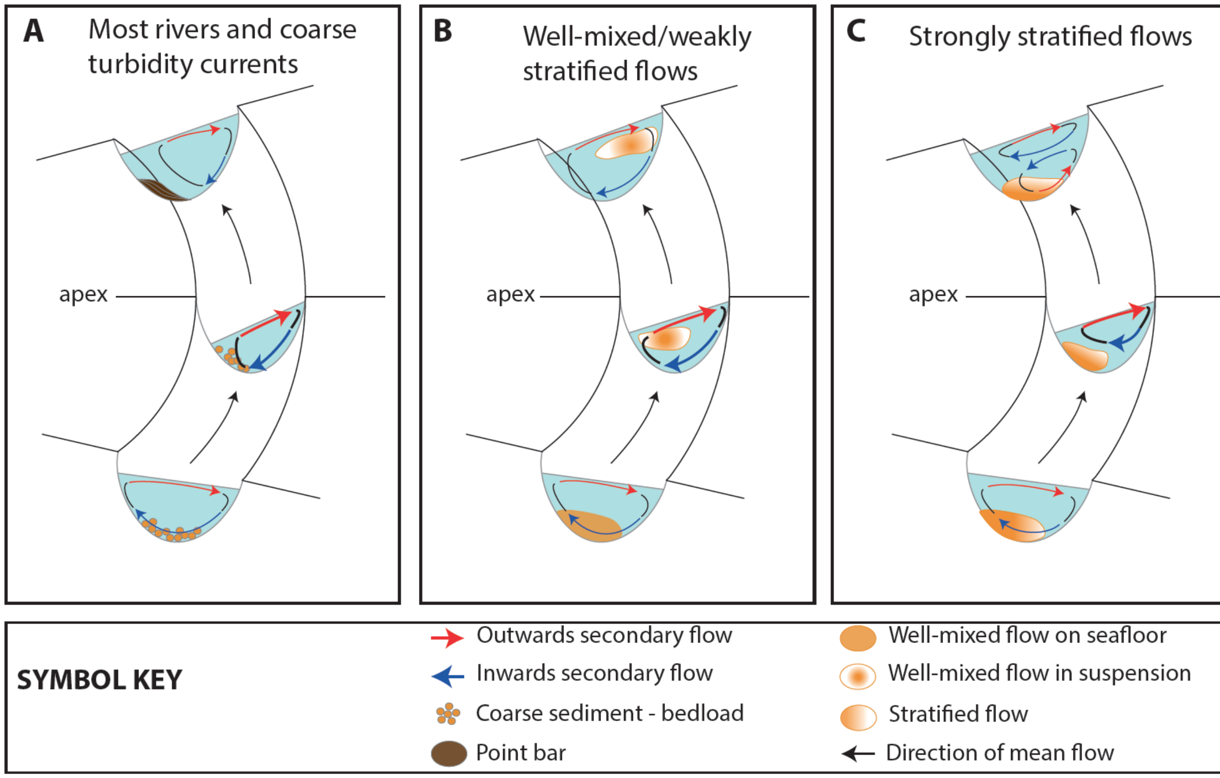

Figure 5. Schematic drawings of resultant secondary velocity in an across-flow section upstream the bend apex, at the bend apex and downstream the bend apex. (a) Model for most rivers and coarse turbidity currents (Scenario A), (b) Model for well-mixed flows (Scenario B) and (c) Model for stratified flows (Scenario C). Thickness of secondary circulation arrows denotes intensity of the flow.

In scenario A, a single weak river-like cell arises where the centrifugally driven pressure gradient displaces sediment to the inner bend as bed load, but has insufficient energy to suspend the sediment; and therefore there is no lateral pressure gradient back across the channel axis (Fig. 5a). We propose that scenario A occurs in bed load-dominated rivers and coarse-grained turbidity current systems, where sediment moves predominantly as bed load and deposits as point bars at the inner bend apex (Bagnold, 1977; Thorne et al., 1985).

In scenario B, a single river-like cell is created. However, in this case the centrifugally driven pressure gradient is sufficient to move and suspend sediment at the inner bend. This results in a lateral pressure gradient that is smaller than that centrifugally driven pressure gradient. The sediment is thus kept in suspension and follows the streamlines of the circulation cell, causing overturning and mixing (Fig. 5b). We propose that scenario B occurs in well-mixed flows such as suspension-dominated rivers and saline flows, where sediment is kept in suspension during the whole process and there is no deposition (Chikita, 1989; Nidzieko et al., 2009).

In scenario C, two circulation cells are formed, with the lower most cell showing river-reversed behaviour. Here, the centrifugally driven pressure gradient pushes sediment towards the inner bend and suspends it sufficiently to generate a lateral pressure gradient back across the channel. When the stratification-triggered pressure gradient is larger than the superelevation-triggered pressure gradient, the cross-stream flow slows down and momentarily stops (Figs. 4, 5c). As the superelevation pressure gradient decrease after the apex, the lateral pressure gradient due to sediment stratification causes suspended sediment to flow back towards the channel axis. This generates a new helical flow cell, beneath the original cell. This bottom cell is river-reversed, and is initiated just downstream of the apex as the centrifugal forces start to decrease. Above the new lower cell, the original river-like cell continues to rotate with a river-like direction (Fig.5c). We propose that scenario C occurs in strongly stratified rivers, saline flows and turbidity currents, where sediment deposits downstream of the bend apex (Chikita, 1989; Nidzieko et al., 2009; Parsons et al., 2010; Darby and Peakall, 2012; Wei et al, 2013).

5.4. Application of the general model to a range of geophysical flows

Our new model is different from previous models (Giorgio Serchi et al., 2011; Dorrell et al., 2013; Peakall and Sumner, 2015) with respect to (i) the location in the channel system where a second basal cell develops, and (ii) the importance of confinement in secondary circulation. In addition it can predict the helical flow structure across a diverse array of particle laden or saline flow types.

Previous work has suggested that direction of rotation of secondary circulation is constant around bends, and changes its rotation direction between adjacent bends. Here we propose that this hypothesis holds for the upper helical flow cell, which is governed by centrifugal forces. However, when a lower helical flow cell develops, this reversed flow cell is generated just downstream of the bend apex. Secondly, we propose that the level of confinement of the channel systems plays an important role in secondary circulation. In confined systems any upper river-like helical flow cell will prevail; whereas in unconfined systems this cell may overspill and thus destroy itself leading to a single river-reversed basal circulation cell (Dorrell et al., 2013).

This study represents a new analysis of the behaviour of the helical structure of submarine flows, and in particular and for the first time, in full-scale oceanic turbidity currents. Our general model applies over a large range of flows spanning from coarse-grained rivers to saline density flows. Here we discuss the implications for understanding the architecture and the evolution of submarine channel systems. In this section we consider the behaviour of multiple flows with the same size and stratification travelling through an evolving channel system. We hypothesize that stratified turbidity currents will behave according to scenario C of our model; in this case near-bed flow is driven towards the outer bend by pressure gradients generated by lateral stratification within the flow. It has previously been suggested (Peakall et al., 2000) that this causes sediment to be deposited as point bars downstream of bend apices. Formation of such a point bar would increase the meander curvature, thus increasing the centrifugal forces and superelevation experienced by subsequent turbidity currents. However, once the pressure gradient towards the inner bend generated by superelevation exceeds the pressure gradient towards the outer bend generated by lateral stratification, then the flow would switch to the behaviour outlined in scenario B. In this case, near-bed flow is driven towards the inner bend by centrifugally-driven pressure gradients. These pressure gradients exceed the lateral stratification-driven pressure gradients. As a consequence, the helical flow overturns sediment in suspension, thereby resulting in no deposition. At this point, the channel would cease meandering and its planform would become locked for flows of such size and stratification.

It is intriguing that the largest submarine fans on Earth are fed by meandering channel systems. We propose that the helical circulation caused by bends, causes sediment to either slosh from side-to-side or to continuously be overturned, thus helping to maintain sediment in suspension over long distances. This mechanism should be considered in addition to turbulence to explain the extraordinary capacity of turbidity currents to transport huge quantities of sediment over hundreds of kilometres.

Acknowledgments

General

We would like to thank Chevron for access to this exceptionally valuable dataset. We also thank Jon Wood (Ocean Data Technology) and others involved in building the mooring and collecting the data.

Funding

M.A. was funded by National Oceanography Centre Southampton and Graduate School of National Oceanography Centre Southampton. M.J.B.C. and P.J.T. were supported by the Natural Environment Research Council projects NE/M017540/1, NE/K011480/1, NE/L009358/1 and NE/M007138/1. D.R.P. recognise funding via HEIF at the University of Hull, and Natural Environment Research Council Project NE/K011480/1. M.A.C. was funded by the natural Environment Research Council grants NE/N012798/1 and NE/P009190/1.

Data and material availability

All data needed to evaluate the conclusions in the paper are presented in the paper and/or the Supporting Information. Additional data related to this paper may be requested from the authors.

References

Abad, J.D., Sequeiros, O.E., Spinewise, B., Pirmez, C., Garcia, M.H. and Parker, G. (2011). Secondary current of saline underflow in a highly meandering channel: experiments and theory. J. Sedim. Res. 81, 787-813.

Azpiroz-Zabala, M., Cartigny, M.J.B., Talling, P.J., Parsons, D.R., Sumner, E.J., Clare, M.A., Simmons, S.M., Cooper, C. and Pope, E., First images of deep-ocean turbidity currents explain sustained flushing of submarine canyons. In press Science Advances.

Bagnold, R.A. (1977). Bed load transport by natural rivers. Water Resour. Res. 13 (2), 303-312.

Bolla Pittaluga, M. and Imran, J. (2014). A simple model for vertical profiles of velocity and suspended sediment concentration in straight and curved submarine channels. Journal of Geophysical Research: Earth Surface 119, 483-503, doi: 10.1002/2013JF002812.

Chikita, K. (1989). A field study on turbidity currents initiated from spring runoffs. Water Resourc. Res. 25 (2), 257-271.

Cooper, C., Wood, J., and Andrieux, O. (2013). Turbidity current measurements in the Congo Canyon. OTC 23992. Offshore Technology Conference, 6-9 May, Houston, Texas. 12 pp.

Cooper, C., Wood, J., Imran, J., Islam, A., Wright, P., Faria, R., Tati, A. and Casey, Z. (2016) Designing for turbidity currents in the Congo Canyon. OTC 26919, Offshore Technology Conference, 2-5 May,

Corney, R.K.T., Peakall, J., Parsons, D.R., Elliot, L., Amos, K.J., Best, J.L., Keevil, G.M. and Ingham, D.B. (2006). The orientation of helical flow in curved channels, Sedimentology 53, 249-257.

Corney, R.K.T., Peakall, J., Parsons, D.R., Elliot, L., Best, J.L , Thomas, R.E., Keevil, G.M., Ingham, D.B. and Amos, K.J. (2008). Reply to Discussion of Imran et al. on ‘‘The orientation of helical flow in curved channels’’ by Corney et al., Sedimentology, 53, 249–257. Sedimentology 55, 241-247.

Cossu, R. and Wells, M.G. (2010). Coriolis forces influence the secondary circulation of gravity currents flowing in large-scale sinuous submarine channel systems. Geophys. Res. Lett., 37, L17603, doi:10.1029/2010GL044296.

Darby, S.E. and Peakall, J. (2012). Modelling the equilibrium bed topography of submarine meanders that exhibit reversed secondary flows. Geomorphology 163-164, 99-109.

Dorrell, R.M., Darby, S.E., Peakall, J., Sumner, E.J., Parsons, D.R. and Wynn, R.B. (2013). Superelevation and overspill control secondary flow dynamics in submarine channels, J. Geoph. Res. 118.

Eggenhuisen, J.T. and Mc Caffrey, W.D. (2012). The vertical turbulence structure of experimental turbidity currents encountering basal obstructions: implications for vertical suspended sediment distribution in non-equilibrium currents. Sedimentology 59, 1101-1120.

Ellison, T.H. and Turner, J.S. (1959). Turbulent entrainment in stratified flows. Journal of Fluid Mechanics 6(3), 423-448. doi: 10.1017/S0022112059000738

Ezz, H. and Imran, J. (2014). Curvature-induced secondary flow in submarine channels, Environ. Fluid Mech. 14, 343-370.

Giorgio Serchi, F., Peakall, J., Ingham, D.B. and Burns, A.D. (2011). A unifying computational fluid dynamics investigation on the river-like to river-reversed secondary circulation in submarine channel bends. J. Geoph. Res., 116, C06012, doi:10.1029/2010JC006361, 2011.

Heezen, B.C., Menzies, R.J., Schneider, E.D., Ewing, W.M., Granelli, N.C.L. (1964). Congo Submarine Canyon. Am. Ass. Petrol. Geol. Bull. 48 (7), 1126-1149.

Huang, H., Imran, J. and Pirmez, C. (2012). The depositional characteristics of turbidity currents in submarine sinuous channels. Marine Geology 329–331, 93–102.

Imran, J., Islam, M.A., Huang, H., Kassem, A., Dickerson, J., Pirmez, C. and Parker, G. (2007). Helical flow couplets in submarine gravity underflows. Geology 35 (7), 659-662.

Imran, J., Islam, M.A., Kassem, A. (2008). ‘‘The orientation of helical flow in curved channels’’ by Corney et al., Sedimentology, Vol. 53, pp. 249–257 – discussion. Sedimentology 55, 235-239.

Islam, M.A. and Imran, J. (2008). Experimental modeling of gravity underflow in a sinuous submerged channel. J. Geoph. Res. 113, C07041, doi:10.1029/2007JC004292.

Janocko, M., Cartigny, M.B.J., Nemec, W. and Hansen, E.W.M. (2013). Turbidity current hydraulics and sediment deposition in erodible sinuous channels: Laboratory experiments and numerical simulations. Mar. and Petrol. Geol. 41, 222-249.

Kassem, A. and Imran, J. (2004). Three-dimensional modeling of density current. II. Flow in sinuous confined and unconfined channels, J. Hydraul. Res. 42 (6), 591-602

Keevil, G.M., Peakall, J., Best, J.L. and Amos, K.J. (2006). Flow structure in sinuous submarine channels: velocity and turbulence structure of an experimental submarine channel, Mar. Geol. 229, 241-257.

Khripounoff, A., Vangriesheim, A., Babonneau, N., Crassous, P., Dennielou, B. and Savoye, B. (2003) Direct observation of intense turbidity current activity in the Zaire submarine valley at 4000 m water depth. Mar. Geol. 194, 151-158.

Nidzieko, N. J., Hench, J.L. and Monismith, S.G. (2009). Lateral circulation in well-mixed and stratified estuarine flows with curvature, J. Phys. Oceanogr., 39, 831–851, doi:10.1175/2008JPO4017.1.

Normark, W.R. (1970). Growth patterns of deep-sea fans. Am. Assoc. Petrl. Geol. Bulletin 54 (11), 2170-2195.

Parsons, D.R., Peakall, J., Aksu, A.E., Flood, R.D., Hiscott, R.N., Besiktepe, S. and Mouland, D. (2010). Gravity-driven flow in a submarine channel bend: direct field evidence of helical flow reversal, Geology 38, 1063-1066.

Peakall, J., McCaffrey, B. and Kneller, B. (2000). A process model for the evolution, morphology, and architecture of sinuous submarine channels. J. Sediment. Res., 70 (3), 434–448.

Peakall, J. and Sumner, E.J. (2015). Submarine channel flow processes and deposits: A process-product perspective. Geomorphology 244, 95-120.

Rozovskii, I.L., 1957. Flow of Water in Bends of Open Channels. Kiev, Academy of Sciences of the Ukrainian SSR, 233 pp.

Savoye, B., Babonneau, N., Dennielou, B. and Bez, M. (2009). Geological overview of the Angola-Congo margin, the Congo deep-sea fan and its submarine valleys, Deep-Sea Res. II 56, 2169-2182.

Shepard, F.P. (1933) Submarine valleys. Am. Geograph. Soc. 23 (1), 77-89.

Sumner, E.J., Peakall, J., Dorrell, R.M., Parsons, D.R., Darby, S.E., Wynn, R.B., McPhail, S.D., Perrett, J., Webb, A. and White, D. (2014). Driven around the bend: Spatial evolution and controls on the orientation of helical bend flow in a natural submarine gravity current, J. Geoph. Res. Oceans 119.

Talling, P.J., Wynn, R.B., Masson, D.G., Frenz, M., Cronin, B.T., Schiebel, R., Akhmetzhanov, A.M., Dallmeier-Tiessen, S., Benetti, S., Weaver, P.P.E., Georgiopoulou, A., Zühlsdorff, C. and Amy, L.A. (2007). Onset of submarine debris flow deposition far from original giant landslide. Nature 450, 541-544.

Talling, P.J., Allin, J., Armitage, D.A., Arnott,R.W.C., Cartigny, M.J.B., Clare, M.A., Felletti, F., Covault, J.A., Girardclos, S., Hansen, E., Hill, P.R., Hiscott, R.N., Hogg, A.J., Hughes Clarke, J., Jobe, Z.R., Malgesini, G.E., Mozzato, A., Naruse, H., Parkinson, S., Peel, F.J., Piper, D.J.W., Pope, E., Postma, G., Rowley, P., Sguzzini, A., Stevenson, C.J., Sumner, E.J., Sylvester, Z., Watts, C. and Xu, J. (2015). Key future directions for research on turbidity currents and their deposits. Journal of Sedimentary Research 85, 153–169. doi: http://dx.doi.org/10.2110/jsr.2015.03

Thorne, C.R., Zevenbergen, L.W., Pitlick, J.C., Rais, S., Bradley, J.B. and Julien, P.Y. (1985). Direct measurement of secondary currents in a meandering sand-bed river. Nature, 316, 746–747.

Umlauf, L. and Arneborg, L. (2009). Dynamics of Rotating Shallow Gravity Currents Passing through a Channel. Part I: Observation of Transverse Structure. J. Phys. Ocean. 39, 2385-2401.

Vangriesheim, A., Khripounoff, A. and Crassous, P. (2009). Turbidity events observed in situ along the Congo submarine channel. Deep-Sea Research II 56, 2208–2222.

Wei, T., Peakall, J., Parsons, D.R., Chen, Z. Zhao, B. and Best, J. (2013). Three-dimensional gravity-current flow within a subaqueous bend: Spatial evolution and force balance variations. Sedimentology 60, 1668–1680.

Supporting Information

Methodology

An acoustic Doppler current profiler (ADCP) was anchored on the canyon thalweg at 2,000 m depth (Fig. 1). The ADCP is an instrument that emits simultaneous acoustic beams to calculate water velocities by Doppler shift. Our instrument was orientated towards the seabed, fixed at 85 m above the seabed (Fig. 1), and it directed its acoustic beams 20° with respect the vertical. It took measurements every 5 seconds from December 2009 to March 2010 within bin sizes of 2 m (Cooper et al., 2013). The ADCP handicap is the loss of measurement quality near the seabed due to the acoustic interference by the seabed. This area, called side lobe interference area (SLIA), covers the first ~5 m above the seabed in this work. We have substituted the velocity measurements in this area by linear extrapolated velocities to zero at seabed level. The maximum velocities have been located in the resulting working dataset. Due to the velocity extrapolation method, flows whose maximum velocities are within the SLIA will show their peak velocity height at the top of this area instead of at the actual height, which is within the unreliable SLIA measured area (Fig. 2 and 3).

Secondary circulation is a balancing flow in a plane perpendicular to the flow direction. Motion towards one side of the plane at certain flow depths is compensated by motion towards the opposite side at the rest of the flow depths. Secondary velocities are the velocity components in this plane, across the depth-averaged flow direction. In our study, the flow depth has been yielded from the integrated system of equations (Ellison and Turner, 1959) that provides flow top distance to the seabed at each time. The seabed has been located by a contrasting high value of echo intensity in a profile of decreasing echo intensity measurements in the water column below the ADCP. The depth-averaged flow direction is calculated from the depth-averages of the North and East components of the velocities given by the ADCP. Secondary velocities towards the outer bend are positive while negative towards the inner bend (Fig. 2b, 2d, 2f and 3).

The calculation of secondary velocity gives values occasionally close to the speed of seawater that has been identified as tidal currents (Fig. 2a, 2c, 2e). Tides strong enough could affect the results of the analysis of secondary circulation. Secondary velocities for the periods when this happens have been removed from the results (Fig. 2b, 2d, 2f).

Depth-profiles of secondary velocities are analysed to identify patterns in the configuration of the secondary circulation. Secondary velocities are calculated for each flow time and arranged by thickness. The average of those values by thickness constitutes the depth-profiles of secondary velocities (Fig. 3a). This process is repeated for each turbidity current and the resultant depth-profiles are averaged into one only profile (Fig. 3b).